

source of water for Earth's oceans (14). This result was anticipated from the high value of O/C in Earth's crust (24), but D/H provides a much stronger argument (14). Mixing of cometary water with water absorbed from the solar nebula by the rocky grains that accreted to form Earth may provide the observed value of (D/H)_{SMOW} (25), as water vapor in the inner solar nebula could have D/H < 1 × 10⁻⁴ (26).

REFERENCES AND NOTES

1. R. Meier *et al.*, *IAU Circ.* 6615 (1997).
2. Line areas are integrated over a velocity interval of ±3 km s⁻¹. Sky noise is the dominant source for the statistical uncertainties of the lines. The ratio of the system temperature in the image and signal sideband was $f = 1.41$. Because the system cannot distinguish between the two sidebands, it scales all lines according to the calibrated upper sideband, which means that the line area of CH₃OH 11₂-11₁ A[±] in the lower sideband has to be multiplied by f . To obtain main beam corrected and absolutely calibrated line areas, the measured antenna temperature has to be divided by the main beam efficiency $\eta = 0.53 \pm 0.05$ and re-scaled by a factor of 1.53 (see text).
3. At 850 μm , the submillimeter common-user bolometer array (SCUBA) of JCMT uses an array of 37 pixels cooled to around 100 mK.
4. N. Biver *et al.*, *Bull. Am. Astron. Soc.* 29, 1047 (1997).
5. N. Dello Russo *et al.*, *ibid.*, p. 1050.
6. D. G. Schleicher, R. L. Millis, T. L. Farnham, S. M. Lederer, *ibid.*, p. 1033.
7. To obtain consistent production rates $Q(\text{CH}_3\text{OH})$, we applied the same model and model parameters to the various measurements. From CSO and IRAM data recorded at the time of the HDO observations, a ratio $Q(\text{CH}_3\text{OH})/Q(\text{H}_2\text{O})$ was derived that agreed with ratios measured with the same telescopes on various occasions in March and April 1997 (4). This fact suggests that the JCMT observations were affected by calibration or pointing problems, although time variability in the cometary activity cannot be excluded.
8. This adjustment is equivalent to the statement that for the purpose of deriving a D/H ratio in water, we compare the $Q(\text{HDO})/Q(\text{CH}_3\text{OH})$ ratio with the $Q(\text{CH}_3\text{OH})/Q(\text{H}_2\text{O})$ ratio derived from CSO and IRAM measurements during March and April. The $Q(\text{HDO})/Q(\text{CH}_3\text{OH})$ ratio does not depend on an absolute calibration. Ratios are only slightly affected by aperture effects, pointing, and comet variability, especially because CH₃OH and H₂O are long-lived species with comparable lifetimes against photodissociation.
9. D. Mehringer *et al.*, *IAU Circ.* 6614 (1997).
10. L. Haser, *Acad. R. Sci. Liege* 43, 740 (1957).
11. J. Crovisier, *J. Geophys. Res.* 99, 3777 (1994).
12. D. Bockelée-Morvan *et al.*, in preparation.
13. N. Biver, thesis, Université Paris VII (1997).
14. P. Eberhardt, M. Reber, D. Krankowsky, R. R. Hodges, *Astron. Astrophys.* 302, 301 (1995); H. Balsiger, K. Altwegg, J. Geiss, *J. Geophys. Res.* 100, 5827 (1995).
15. R. Hagemann, G. Nief, E. Roth, *Tellus* 22, 712 (1970); J. P. De Witt, C. M. Van der Straaten, W. G. Mook, *Geostand. Newsl.* 4, 33 (1980).
16. For example, M. E. Bailey *et al.* [*Mon. Not. R. Astron. Soc.* 281, 916 (1996)] conducted extensive numerical simulations on the orbital evolution of Hale-Bopp.
17. H. F. Levison and M. J. Duncan, *Icarus* 108, 18 (1994).
18. J. H. Oort, *Bull. Astron. Inst. Neth.* 11, 91 (1950); P. R. Weissman, in *Comets in the Post-Halley Era*, R. L. Newburn *et al.*, Eds. (Kluwer Academic, Dordrecht, Netherlands, 1991), vol. 1, pp. 463–486.
19. R. D. Gensheimer, R. Mauersberger, T. L. Wilson, *Astron. Astrophys.* 314, 281 (1996).

20. T. J. Millar, A. Bennett, E. Herbst, *Astrophys. J.* 340, 906 (1989).
21. P. D. Brown and T. J. Miller, *Mon. Not. R. Astron. Soc.* 237, 661 (1989).
22. J. L. Lunine, S. Engel, B. Risz, M. Horanyi, *Icarus* 94, 333 (1991).
23. W. M. Irvine and R. F. Knacke, in *Origin and Evolution of Planetary and Satellite Atmospheres*, S. K. Atreya, J. B. Pollack, M. S. Matthews, Eds. (Univ. of Arizona Press, Tucson, 1989), pp. 3–34.
24. T. C. Owen and A. Bar-Nun, *Icarus* 116, 215 (1995).
25. T. Owen, in *From Stardust to Planetesimals*, Y. J. Pendleton and A. G. G. M. Tielens, Eds. (ASP Publ. 122, Astronomical Society of the Pacific, San Francisco, 1997), pp. 435–450.
26. C. Lecluse and F. Robert, *Geochim. Cosmochim. Acta* 58, 2927 (1994).

27. We thank M. Mumma and N. Dello Russo for providing us with H₂O production rates before publication, D. G. Schleicher for helpful discussion of his prepublication OH observations, the operators of JCMT for their assistance, P. Eberhardt for valuable comments on the manuscript, and B. Marsden and D. Tholen for help with the ephemerides. This work was supported by NASA grants NAEW 2650 and NAEW 2631. D.C.J. acknowledges support from NSF grant AST96-15603. The JCMT is operated by the Joint Astronomy Centre on behalf of the Particle Physics and Astronomy Research Council of the United Kingdom, the Netherlands Organisation for Scientific Research, and the National Research Council of Canada.

2 October 1997; accepted 29 December 1997

Water in Betelgeuse and Antares

Donald E. Jennings*† and Pedro V. Sada*

Absorption lines of hot water have been identified in the infrared spectra of Betelgeuse (α Orionis) and Antares (α Scorpii) near 12.3 micrometers (811 to 819 wavenumbers). The water lines originate in the atmospheres of the stars, not in their circumstellar material. The spectra are similar in structure to umbral sunspot spectra. Pure rotation water lines of this type will occur throughout the spectra of cool stars at wavelengths greater than 10 micrometers. From the water spectra, the upper limit for the temperature in the line formation region in both stars is 2800 kelvin. The water column density in both stars is $(3 \pm 2) \times 10^{18}$ molecules per square centimeter, yielding an abundance relative to atomic hydrogen of $n(\text{H}_2\text{O})/n(\text{H}) \approx 10^{-7}$.

Water is abundant in cool stars (1) and is a major molecular constituent at low temperatures in oxygen-rich stars, dominating all molecules other than CO and H₂ in regions at temperatures below 2000 K (2). The spectrum of hot water is most commonly observed in the near infrared at wavelengths between 0.9 and 3.2 μm (3–5). In M-type stars, strong H₂O absorption is seen in Mira-type variables, whereas non-variable stars have weaker or no water absorption [see (3), for example]. Recently, water was detected in sunspots (6), where the temperature can be as low as in M-type stars. Water dominates the spectrum in sunspots at 10 to 20 μm , as identified from laboratory studies of water spectra taken at high temperatures (6–8). At 3000 to 4000 K, sunspots provide a starting point in a search for hot water in stars cooler than the sun, even though the physical conditions other than temperature are different. The improved understanding of sunspot spectra, plus the laboratory and theoretical characterization of the pure-rotation region of hot

water, motivated us to obtain spectra of M-type supergiants.

Betelgeuse [α Orionis (α Ori, class M1-2 Ia-Iab)] and Antares [α Scorpii (α Sco, M1.5 Iab-Ib)] are among the brightest late M-type supergiants. They are both oxygen-rich with visible effective temperatures near 3500 K (9). They also both exhibit the extended atmospheres typical of red supergiants and have circumstellar dust shells with inner radii of more than 25 stellar radii (10) and mass loss rates of 10⁻⁶ to 10⁻⁵ solar masses per year (11). Both undergo irregular or semiregular variability.

Betelgeuse (α Ori) is the brightest and most studied M-type supergiant. The continuum flux from this star at 12 μm is a combination of radiation from the chromosphere at about 3200 K (12) and a circumstellar dust shell at about 500 K (13). The star's magnitude at 12 μm is -5.5 (14); it is a semiregular variable with a recent visual luminosity range between magnitudes 0.3 and 0.9 and a period of about 6 years (12). It changes by 0.1 magnitude at 11 μm during a period (12). Both CO and SiO are observed in the circumstellar envelope (15), but water was not reported in spectra of this star (16), and it has been used as a water-free reference source (4).

Antares (α Sco) has a binary companion, a fainter dwarf B-type star with a separation of 2.9 arc sec. The visual magni-

D. E. Jennings, Planetary Systems Branch, Code 693, NASA Goddard Space Flight Center, Greenbelt, MD 20771, USA.

P. V. Sada, Consultoría Astronómica de Monterrey, Bosques de Pirineos 520-3, Col. Bosques del Valle, Garza García, N.L. 66250, México.

*Visiting Astronomer, National Solar Observatory, Tucson, AZ 85726, USA.

†To whom correspondence should be addressed.

Table 1. Measurements of water in α Ori and α Sco. Observed line positions, peak absorptions, and equivalent widths for both H_2O and OH are listed for the two stars. The frequencies and assignments for the H_2O transitions are

from (7); assignments are written $J'_{Ka'Kc'} - J_{KaKc}$ (0v0); dash means the line is not assigned. The other numbers in parentheses are the 1σ errors in the least significant digits.

Rest line frequency (cm ⁻¹)		Transition assignment	Star	Observed line frequency (cm ⁻¹)	Peak absorption	Observed equivalent width (cm ⁻¹)	Corrected equivalent width* (cm ⁻¹)	
811.176	H ₂ O	19 _{16 3} - 18 _{15 4} (030)	†	α Sco	811.18(2)	0.031(5)	0.0039(6)	
811.203	H ₂ O	—						
811.560	H ₂ O	22 _{15 7} - 21 _{14 8} (000)	†	α Ori	811.53(2)	0.044(3)	0.0052(4)	
								α Sco
811.690	H ₂ O	20 _{15 6} - 19 _{14 5} (020)	†	α Sco	811.68(3)	0.072(5)	0.0087(6)	
811.933	H ₂ O	21 _{15 6} - 20 _{14 7} (010)						α Ori
811.965	H ₂ O	23 _{13 10} - 22 _{12 11} (000)	†	α Sco	811.93(2)	0.098(5)	0.0122(6)	
811.980	H ₂ O	21 _{15 7} - 20 _{14 6} (010)						
815.301	H ₂ O	18 _{7 12} - 17 _{4 13} (000)	‡	α Ori	815.35(2)	0.051(15)	0.0061(15)	
				α Sco	815.33(4)	0.120(30)	0.0150(24)	
815.400	OH	R ₂₆ (23.5)		α Ori	815.41(2)	0.037(15)	0.0034(15)	0.0052(25)
				α Sco	815.43(4)	0.083(30)	0.0077(24)	0.0118(40)
815.949	OH	R ₁₁ (24.5)	α Ori	815.95(2)	0.038(10)	0.0034(10)	0.0052(15)	
			α Sco	815.92(3)	0.080(10)	0.0074(12)	0.0114(25)	
816.155	H ₂ O	22 _{13 10} - 21 _{12 9} (010)	†	α Sco	816.13(3)	0.047(10)	0.0040(12)	
818.424	H ₂ O	22 _{16 6} - 21 _{15 7} (000)						α Ori

*Corrected for 35% flux contribution from circumstellar emission. †Observed feature was a blend of these H₂O transitions. ‡Blend of H₂O and OH lines; separate positions within features were estimated.

tudes of the two stars are 1 and 5, and at 12 μ m the dwarf companion did not contribute measurably to our observed flux. The magnitude of α Sco at 12 μ m is -4.7 (14). In the visible, it varies in the range 0.9 to 1.8 magnitudes with a 4.7-year period (17). Its variation is not well characterized at 12 μ m but is probably small (12). Like α Ori, α Sco contains CO in its circumstellar shell (18). There has also been no previous report of water in the atmosphere of α Sco.

Molecular lines formed in chromospheres serve as probes of stellar structure and dynamics. Atmospheric structure in cool stars is driven by the opacities of molecules, principally water (19). The relatively low dissociation temperature of many molecules causes them to be present only in the cooler portions of stellar atmospheres. When its spectrum is well characterized, the rotational temperature of an atmospheric molecule can be measured from relative line intensities. Also, variability in radial velocity and temperature in stellar atmospheres can be tracked by means of changes in line positions and intensities. In variable stars, the structure of the spectrum of water can be expected to change with luminosity [see (4), for example]. Observations in the far-infrared region can take advantage of the lower opacity of circumstellar material at longer wavelengths.

The spectra of α Ori and α Sco (Fig. 1) were recorded using a high-resolution cryogenic grating spectrometer (20) on the McMath-Pierce Telescope at Kitt Peak (21). We observed α Ori on 21 to 25 March 1997 and α Sco on 21 to 23 May 1997. The regions near 811.5 and 815.5 cm⁻¹ were observed in both stars. An additional region

near 818.0 cm⁻¹ was observed in α Ori. A sunspot umbral spectra (22) provided an example of high-temperature water for comparison with α Ori and α Sco, but our identification of water in these stars is based entirely on comparison with laboratory data (7, 23).

All of the transitions (Table 1) are purely rotational and occur in the ground or excited states. Observed frequencies of the unblended lines fall within measurement uncertainties, which were limited by the accuracy of the terrestrial CO₂ and H₂O calibration and the noise in each line. Peak line absorptions were measured with respect to the continuum level in each spectrum. The integrated line intensities are listed as equivalent widths. These equivalent widths were then corrected for an estimated 35% contribution of 12- μ m flux from the extended circumstellar shell of each star within our slit. This fraction of circumstellar radiation is consistent with other results for α Ori (24) and α Sco (25). A degradation in the accuracy of the corrected equivalent widths is due to an additional 10% uncertainty in the flux from the shells. We observed the line at 811.56 cm⁻¹ in α Ori in 1985 and identified it as due to Mg I (un-ionized Mg) (26); another unidentified line was seen near 811.95 cm⁻¹. Both of these lines are due to water. The OH lines were also detected previously in α Ori (26).

Our water spectra in α Ori and α Sco are similar in overall appearance, but the detailed spectral structure in the two stars is different. The lines in α Sco are generally stronger, with the peak absorption reaching $\sim 10\%$, as compared with $\sim 5\%$ in α Ori. Also, some features appear in α Sco that do

not appear in α Ori. Just as in sunspots (22), the water spectrum in the 10- to 20- μ m region in these two stars will be dense with lines. At low spectral resolution, water contributes a small opacity to the far-infrared spectra of this type of star. We did not resolve the Doppler widths of the lines at our resolution. The linewidths observed for α Ori in (26), corrected for instrumental broadening, correspond to a turbulent velocity of 12 km s⁻¹. For α Sco, the velocity was reported to be as high as 16 km s⁻¹ (27). When convolved with the instrumental width of 0.1 cm⁻¹, this velocity gives linewidths that are consistent with our observations.

The relative strengths at high temperatures of the H₂O lines we observed are not known well enough to derive atmospheric temperatures from our data. However, we can find upper limits of temperature and derive abundance estimates. In the line formation regions of these atmospheres, the partial pressure of H₂O increases rapidly with decreasing temperature [see figure 3 of (2)]. We therefore adopted a single-layer, plane-parallel, isothermal model [see, for example, (4)] in which these lines are formed in the region of high water abundance. This is the region above the level where the temperature is low enough for water to form and below the level where the total pressure is so low that the water abundance becomes negligible. This layer will probably be near the temperature minimum (T_{\min}) in the lower chromosphere of the star (28), if such a minimum exists. This single-layer model is an approximation that assumes uniformity in three dimensions within the layer, including across the stellar disk (29). Within the lim-

itations of our incomplete knowledge of hot water line intensities, our small data set, and uncertainties in the atmospheric structure, this approach produced abundances that could be compared with predictions for these stars.

We assumed that the depths of the stron-

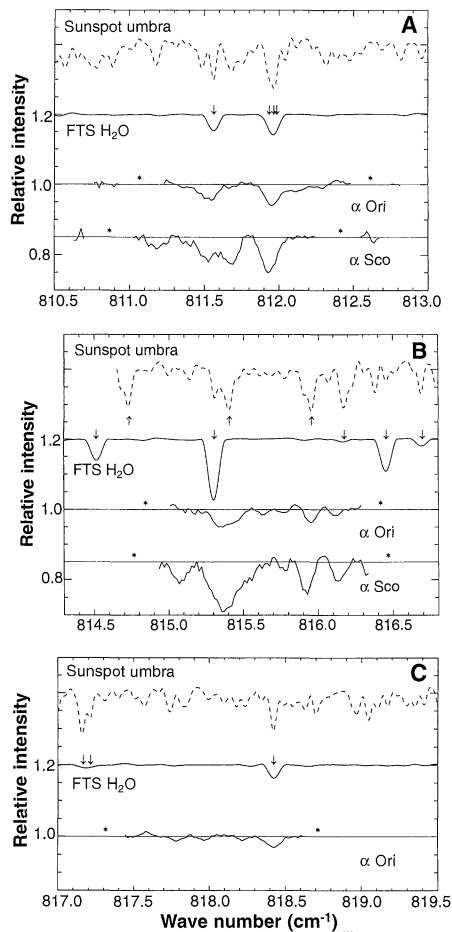


Fig. 1. The observed spectra of water in the two M-type supergiant stars Betelgeuse (α Ori) and Antares (α Sco). Three regions are displayed, near (A) 811.5 cm^{-1} , (B) 815.5 cm^{-1} , and (C) 818.0 cm^{-1} . Spectra of α Ori are shown in all three; α Sco was observed in regions (A) and (B) only. The intensity scale is for the spectrum of α Ori, and the spectrum of α Sco is shifted down by 0.15. A sunspot umbral spectrum (3200 K) and a laboratory spectrum of hot water [McMath-Pierce Telescope's Fourier transform spectrometer (FTS), 1300 K] are shown (22, 23). The laboratory spectrum was recorded with 0.9-torr H_2O . It is an emission spectrum, which we display upside down for comparison with the stellar absorption spectra. The stellar and laboratory spectra were smoothed to match the 0.1 cm^{-1} resolution of the spectrometer. The sunspot umbral spectrum was smoothed to 0.05 cm^{-1} . Prominent H_2O lines are indicated with downward arrows above the laboratory spectra. OH lines are indicated with upward arrows below the sunspot spectra. Sections in the stellar spectra indicated by asterisks are where lines of terrestrial CO_2 [in (A) and (C)] and H_2O [in (B)] were present.

ger lines approach the saturated absorption levels (high optical depth) within the layer and therefore provide an upper limit for the temperature of the layer (T_L). We also assumed that the continuum level in each spectrum corresponds to the effective temperature T_{eff} of the star. To represent line saturation, we assigned an optical depth of unity to the peak absorption of the strong feature at 811.95 cm^{-1} . After correcting for 35% circumstellar flux, our upper limit for T_L/T_{eff} is 0.86 for α Ori and 0.76 for α Sco. The 11- μm effective temperatures are 3190 and 3500 K, respectively (12). The resulting upper limits are not significantly different in the two stars, within the limits of our derivation, and we place the temperature at $T_L < 2800$ K. This value can be compared with $T_{\text{min}} = 2700$ K derived from ultraviolet observations of α Ori (28).

The abundance of water in the stars can be estimated from the known strength of the 815.30 cm^{-1} line. This line is the only one we observed whose strength is tabulated in the available database (30). The line was corrected for blending with the neighboring OH line in our spectra. We calculated the high-temperature absorption intensity of this line by using the temperature dependence $Q(T)^{-1} \exp(-E_L/kT)$ for the population of the lower energy level E_L , where $Q(T)$ is the partition function calculated from tabulated thermodynamic properties of water (31) (k is the Boltzmann constant). We used the range 2500 to 2800 K to represent our uncertainty in the temperature of the line formation regions in the stars. The derived line strength for the 815.30 cm^{-1} line is $(3.0 \pm 0.2) \times 10^{-20}$ cm^{-1} per molecule per square centimeter. From our corrected equivalent widths for this line (Table 1), we find that the column densities are similar in the two stars, with a value $(3 \pm 2) \times 10^{-18}$ cm^{-2} . The fractional abundance $n(\text{H}_2\text{O})/n(\text{H})$ can be obtained from an estimate of the column density of atomic hydrogen in the H_2O line formation region. We obtained a column density of 3×10^{25} cm^{-2} for H in α Ori by integrating the layers listed in table 9 of (28) for temperatures below 3000 K. The ratio of the column densities of H_2O and H gives $n(\text{H}_2\text{O})/n(\text{H}) \approx 10^{-7}$. This calculation agrees with the prediction presented in figure 3 of (2) for ~ 2700 K atmospheres of oxygen-rich supergiants.

Some differences are apparent in the detailed structure of the water spectra in the two stars. Although our limited spectral coverage and sensitivity make a rigorous comparison impossible, these differences are probably the result of dissimilar temperature and abundance profiles in the two stellar atmospheres. In particular, the line at 811.68 cm^{-1} appears stronger in α Sco than in α Ori, compared with the neigh-

boring 811.52 and 811.94 cm^{-1} lines. This line is also stronger in the ~ 3200 K sunspot spectrum compared with the ~ 1300 K laboratory spectrum (Fig. 1). The differences may result from the higher vibrational level of the 811.68 cm^{-1} transition (Table 1), which makes this line relatively more intense at higher temperatures.

These stars will have water absorption in other portions of their spectra, particularly in the 2- μm region. In the case of α Ori, which has been observed at 2.0 to 2.4 μm at high spectral resolution (32), there was no report of water. In α Ori and α Sco, the water lines will be weak near 2 μm , because of the low water abundances at their temperatures and the fact that water transitions at 2 μm are intrinsically much weaker than those at 12 μm . From our derived column density, we have calculated equivalent widths for strong lines at 2 μm in α Ori to be $< 5 \times 10^{-4}$ cm^{-1} , implying that these lines will be less than 1% deep. This value is below the achieved detection limit, explaining why they have not been seen. New observations in the near infrared, with the improved sensitivity available with current spectrometers, are certainly needed for a comprehensive treatment of water in these stars.

REFERENCES AND NOTES

1. L. H. Aller, in *Stellar Atmospheres*, J. L. Greenstein, Ed. (Univ. of Chicago Press, Chicago, 1960), pp. 252-257.
2. T. Tsuji, *Ann. Tokyo Astron. Obs.* **9**, 1 (1964).
3. H. Spinrad and R. L. Newburn, *Astrophys. J.* **141**, 965 (1965).
4. K. H. Hinkle and T. G. Barnes, *ibid.* **227**, 923 (1979).
5. F. Allard, P. H. Hauschildt, S. Miller, J. Tennyson, *ibid.* **426**, L39 (1994); T. Tsuji, K. Ohnaka, W. Aoki, I. Yamamura, *Astron. Astrophys.* **320**, L1 (1997).
6. L. Wallace *et al.*, *Science* **268**, 1155 (1995).
7. O. L. Polyansky, J. R. Busler, B. Guo, K. Zhang, P. F. Bernath, *J. Mol. Spectrosc.* **176**, 305 (1996). Updated H_2O data were provided by an anonymous referee.
8. O. L. Polyansky *et al.*, *Science* **277**, 346 (1997).
9. G. P. Di Benedetto, *Astron. Astrophys.* **270**, 315 (1993).
10. G. C. Sloan, G. L. Grasdale, P. D. LeVan, *Astrophys. J.* **404**, 328 (1993); E. E. Bloemhof and R. M. Danen, *ibid.* **440**, L93 (1995).
11. N. Maun, *Astron. Astrophys.* **227**, 141 (1990); K. A. van der Hucht, A. P. Bernat, Y. Kondo, *ibid.* **82**, 14 (1980).
12. M. Bester *et al.*, *Astrophys. J.* **463**, 336 (1996).
13. K. G. Carpenter, R. D. Robinson, G. M. Wahlgren, J. L. Linsky, A. Brown, *ibid.* **428**, 329 (1994).
14. D. Y. Gezari, M. Schmitz, J. M. Mead, in "Far Infrared Supplement: Catalog of Infrared Observations," *NASA Ref. Publ.* 1119 (May 1984).
15. A. P. Bernat, D. N. B. Hall, K. H. Hinkle, S. T. Ridgway, *Astrophys. J.* **233**, L135 (1979); S. T. Ridgway, D. F. Carbon, D. N. B. Hall, J. Jewell, *Astrophys. J. Suppl. Ser.* **54**, 177 (1984).
16. R. Beer, R. B. Hutchison, R. H. Norton, D. L. Lambert, *Astrophys. J.* **172**, 89 (1972).
17. D. Hoffleit and C. Jaschek, *The Bright Star Catalog* (Yale Univ. Observatory, New Haven, CT, ed. 4, 1982), p. 422.
18. T. P. Snow Jr., R. H. Buss Jr., D. P. Gilra, J. P. Swings, *Astrophys. J.* **321**, 921 (1987).
19. T. Tsuji and K. Ohnaka, in *Elementary Processes in*

- Dense Plasmas*, S. Ichimaru and S. Ogata, Eds. (Addison-Wesley, Reading, MA, 1995), pp. 193–200.
20. D. E. Jennings *et al.*, in *Infrared Solar Physics*, D. Rabin *et al.*, Eds. (Kluwer Academic, Dordrecht, Netherlands, 1992), pp. 151–160.
 21. Our grating spectrometer is liquid-helium cooled and is designed to operate in the 5- to 28- μm wavelength range. The grating dimensions are 18 cm by 33 cm, and it is ruled with 31.6 grooves per millimeter. A circular variable filter was used to select the fourth diffraction order of the grating at 12 μm . This spectrometer uses a 128 by 128 blocked impurity band (BIB) Si:As detector array. The slit width was chosen to give a spectral resolution of about 0.1 cm^{-1} . Spectra of the moon and Mars were used to calibrate the instrument response and to establish the frequency scale in each spectrum with the use of terrestrial CO_2 and H_2O absorption lines.
 22. L. Wallace, W. Livingston, P. F. Bernath, "An Atlas of the Sunspot Spectrum from 470 to 1233 cm^{-1} (8.1 to 21 μm) and the Photospheric Spectrum from 460 to 630 cm^{-1} (16 to 22 μm)," *National Solar Observatory Tech. Rep. 1994-01* (1994).
 23. P. F. Bernath, archived spectra of the National Solar Observatory, spectrum #50, recorded 04/09/93 (1993).
 24. R. Treffers and M. Cohen, *Astrophys. J.* **188**, 545 (1974).
 25. M. L. Cobb and J. D. Fix, *ibid.* **315**, 325 (1987).
 26. D. E. Jennings, D. Deming, G. R. Wiedemann, J. J. Keady, *ibid.* **310**, L39 (1986).
 27. A. de Koter, C. de Jager, H. Nieuwenhuijzen, *Astron. Astrophys.* **200**, 146 (1988).
 28. G. S. Basri, J. L. Linsky, K. Eriksson, *Astrophys. J.* **251**, 162 (1981).
 29. If the star has "starspots," cool areas analogous to sunspots, the distribution of H_2O will be patchy within our beam. There is evidence that the disk of α Ori is not uniform in brightness [see, for example, V. A. Klückers, M. G. Edmunds, R. H. Morris, N. Woeder, *Mon. Not. R. Astron. Soc.* **284**, 711 (1997)]. If the water exists in localized areas, a model using a filling factor for water, rather than a uniform chromospheric layer, would be more appropriate. Observationally, a nonuniform distribution of water might make it possible to detect changes in the spectra as the star rotates.
 30. L. S. Rothman *et al.*, *Appl. Opt.* **26**, 4058 (1987).
 31. *JANAF Thermochemical Tables* (Dow Chemical, Midland, MI, 1965). Calculation methods are described by G. N. Lewis and M. Randall, *Thermodynamics* (McGraw-Hill, New York, 1961), p. 419.
 32. L. Wallace and K. Hinkle, *Astrophys. J. Suppl. Ser.* **107**, 312 (1996).
 33. The authors thank P. Bernath, K. Hinkle, and L. Wallace for supplying preprints; D. Deming, D. Reuter, and G. McCabe for discussions; R. Boyle, K. McFarland, and E. Zamkoff for assisting during the observations; G. Bjoraker for supplying line strengths; and the staff of the National Solar Observatory. The National Solar Observatory is a division of the National Optical Astronomy Observatories, which is operated by the Association of Universities for Research in Astronomy, under contract with the National Science Foundation. Celeste was manufactured by IR Systems, and its electronics were manufactured by Wallace Instruments. The BIB detector array was manufactured by Boeing Research and Technology Center.

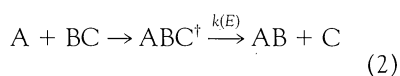
18 September 1997; accepted 15 December 1997

Femtosecond Activation of Reactions and the Concept of Nonergodic Molecules

Eric W.-G. Diau, Jennifer L. Herek,* Zee Hwan Kim, Ahmed H. Zewail

The description of chemical reaction dynamics often assumes that vibrational modes are well coupled (ergodic) and redistribute energy rapidly with respect to the course of the reaction. To experimentally probe nonergodic, nonstatistical behavior, studies of a series of reactions induced by femtosecond activation for molecules of varying size but having the same reaction coordinates $[\text{CH}_2 - (\text{CH}_2)_{n-2} - \text{C} = \text{O}^\dagger \rightarrow \text{products}]$, with $n = 4, 5, 6$, and 10] were performed. Comparison of the experimental results with theoretical electronic structure and rate calculations showed a two to four orders of magnitude difference, indicating that the basic assumption of statistical energy redistribution is invalid. These results suggest that chemical selectivity can be achieved with femtosecond activation even at very high energies.

The concept of ergodicity in molecules is central to chemical reactivity. Given the complexity of molecules with numerous degrees of freedom, vibration, and rotation, how would a deposited energy (E) redistribute, and how does such behavior of intramolecular vibrational-energy redistribution (IVR) affect the subsequent chemical reaction? These questions have been addressed, starting in the 1920s and 1930s, by Lindemann (1) and Hinshelwood (2), among others, and have become the key to the assumptions in theories of unimolecular and complex-forming bimolecular reactions:



where A, B, and C are molecules, the dagger indicates activated molecules, and k is the microcanonical rate coefficient of E . If the system is nonergodic, the vibrational motions are not coupled and reactivity may be described by a nonstatistical theory such as that of Slater (3). If all modes are coupled, ergodicity prevails and the statistical Rice-Ramsperger-Kassel-Marcus (RRKM) theory (4) becomes the appropriate description.

Probing of IVR behavior and $k(E)$ is convoluted by the process of preparation of the molecule, which defines the energy distribution of states, by the method of measurement, and by the time scale of IVR relative to the time of the reaction. In a conventional collisional activation of a reaction by the Lindemann mechanism (that is, by collisions between A and a partner molecule M to produce A^\dagger), the collisions prepare a broad energy distribution, and it is difficult to ascertain the time scales involved. Rabinovitch and colleagues (5, 6), in a classical series of papers on chemical

activation ($A + BC$), secured a narrower energy distribution, making it possible to infer the time for energy redistribution in ABC^\dagger before product formation of $AB + C$.

Such an approach to chemical activation has been studied in bulk and in molecular beams; in bulk studies, $k(E)$ has been inferred from measurements of product yield with the frequency of deactivating collisions as an estimating clock. At the high vibrational energies, in excess of a reaction threshold of 30 to 40 kcal/mol, the description (5, 6) was in favor of ergodic, statistical behavior for molecules with lifetimes longer than about 100 ps. This proposition has been challenged over the years (7). For most systems, it appears that ergodic behavior prevails at relatively high energies.

The experimental search for a quantitative measure of ergodic behavior has involved different approaches. Studies of the decomposition of molecular ions (acetone cation) have shown deviations from the statistical behavior (8). Real time studies of $k(E)$ under controlled preparation of A^\dagger , in a molecular beam, by ultrashort laser pulses have shown that, for an isomerization reaction with a barrier of 3 to 4 kcal/mol, IVR is restricted among a select number of states (9). Similarly, for van der Waals molecules, the predissociation dynamics has been shown to be non-RRKM (10). Theoretical studies have addressed the nature of selective IVR and its effect on reaction rates and spectral (CH overtones) line shapes (11, 12).

A variety of calculational and experimental work has been devoted in recent years to this subject and its relevance to the so-called regular or chaotic motion, the transition from statistical to nonstatistical behavior, and the important subject of energy flow and bond selective chemistry (13, 14). It was recognized early (15) that devi-

Arthur Amos Noyes Laboratory of Chemical Physics, California Institute of Technology, Pasadena, CA 91125, USA.

*Present address: Department of Chemical Physics, Lund University, Lund, Sweden.